Detailed Kinetic Modeling of Gas-Phase Reactions in the Chemical Vapor Deposition of Carbon from Light Hydrocarbons

Koyo Norinaga*,† and Olaf Deutschmann

Institut für Technische Chemie und Polymerchemie, Universität Karlsruhe, Engesserstrasse 20, 76131 Karlsruhe, Germany

The chemical kinetics of the pyrolysis of the hydrocarbons ethylene, acetylene, and propylene are modeled in detail under conditions relevant to the chemical vapor deposition of pyrolytic carbon. A mechanism that consisted of 227 species and 827 reactions (most of which are reversible) is developed and computed using a software package designed for computing time-dependent homogeneous reaction systems. Experimental results used for model validation are obtained using a vertical flow reactor at 900 °C, pressures of 2−15 kPa, and residence times of up to 1.6 s. The products are analyzed using on-line and off-line gas chromatography. Computational and experimental results are compared for more than 30 products, including hydrogen, small hydrocarbons (ranging from methane to C_4 species), and aromatic hydrocarbons (ranging from benzene to coronene). The resulting reaction model predicts the profiles of the major pyrolysis products (mole fractions of $>10^{-2}$) of the three hydrocarbons, as a function of both residence time and pressure, with satisfactory accuracy. It also predicts the mole-fraction profiles of minor compounds, ranging from polycyclic aromatic hydrocarbons (PAHs) to naphthalene, fairly well; however, it significantly underpredicts the larger PAHs. The deviation increases as the molecular mass of the PAHs increases. Sensitivity and reaction-rate analyses were also conducted to identify crucial reaction steps.

1. Introduction

Pyrolytic carbon production via chemical vapor deposition (CVD) is one of the most important processes in carbon materials technology, especially for carbon fiber-reinforced carbon (C/C) composites.[1,2] Isobaric and isothermal chemical vapor infiltration (CVI) of carbon is an accepted process for the synthesis of C/C composites used in the aerospace industry for rockets, missile nozzles, and brake disks. In the CVI of carbon, the following processes proceed simultaneously and interdependently: (1) homogeneous gas-phase pyrolysis of light hydrocarbons (generally methane,[3] propane,[4,5] and propylene[6]); (2) transportation of gaseous species inside a fibrous preform; and (3) heterogeneous reactions yielding solid deposits that densify the preform. Gas-phase reactions form a great variety of hydrocarbons and hydrocarbon radicals, and any of these species has the potential to chemisorb or physisorb at the growing pyrolytic carbon surface. The chemistry underlying carbon CVD and CVI has been obscured by the complexity of the mechanism, which involves both the gas phase and surface.

Mathematical models[7−12] have been increasingly applied to understand the CVD and CVI of carbon more precisely. Appropriate models must incorporate chemical reaction schemes and all of the transport phenomena involved. Becker and Hüttinger[10] have proposed a simplified model that predicts the kinetics of carbon deposition from C_2 hydrocarbons. In their model, seven parameters, including five adjustable reaction-rate constants, are used to fit only two observables: deposition rate and residence time. In addition, a large number of gas-phase species are lumped into three groups: C_2, C_4, and C_6 hydrocarbons. Transport phenomena are not considered, and the deposition reactions are treated using simple first-order reaction constants. This simplified model is a good benchmark for further studies, including simulations of the CVI process;[11,12] however, as it stands, it explains experimental results for only a limited range of conditions and gives little insight into the CVD of carbon at a molecular level.

To understand these chemical reaction processes more precisely, a detailed chemical kinetic-modeling approach is needed, rather than the "lumped" approach of Becker and Hüttinger. In the more-sophisticated approach, hundreds of elementary reactions are compiled, and the governing equations for a given system are solved numerically. The parameters that must be considered are the system parameters, such as temperature, pressure, time, and initial reactant concentrations, and the kinetic parameters for each chemical reaction. Assuming an Arrhenius-like rate expression, the pre-exponential, temperature exponent, and activation energy must be known for every elementary reaction. The kinetic parameters are intrinsic to the chemical reactions and can be derived experimentally or from theoretical calculations. Therefore, in principle, a model developed using this approach would involve no adjustable or fitting parameters and could be used under a wide range of conditions.

Detailed chemical kinetic modeling for light hydrocarbons pyrolysis were extensively performed,[13−27] of which a few studies were concerned with the CVD of carbon.[25−27] Ziegler et al.[26,27] proposed a reaction mechanism for propane pyrolysis under conditions relevant to the CVI process. They evaluated their mechanism by comparing the computational and experimentally determined data for a perfectly stirred reactor at 900−1025 °C with a residence time of 0.5−3.0 s and a propane pressure of 0.35 kPa. Twenty-nine products were analyzed, ranging from hydrogen to pyrene. Considering the wide range of temperature and residence time, the agreement between the computational and experimental results was quite satisfactory. This mechanistic study was limited to propane pyrolysis at one pressure; however, the pressure or initial concentration of a reactant is an important operational variable in the CVD[28] and CVI[29] of carbon. In the present study, we attempted to develop

* To whom correspondence should be addressed. Tel.: +81-11-706-6841. Fax: +81-11-726-0731. E-mail: norinaga@eng.hokudai.ac.jp.

† Current address: Center for Advanced Research of Energy Conversion Materials, Hokkaido University, N13-W8, Kitaku, Sapporo, 060-8628, Japan.

10.1021/ie061207p CCC: $37.00
Published on Web 04/07/2007

a more-comprehensive mechanism that predicts the pyrolysis behaviors of three hydrocarbons, covering the formation profiles of a wide range of products. Rather than a manual mechanism model development, the computationally generating mechanism approaches[15,17,20,30−35] would be suitable for modeling such a complex system of hydrocarbon pyrolysis. However, these automated methods are not mature enough to handle the chemistry of larger species such as polycyclic aromatic hydrocarbons (PAHs), which are important precursors of pyrolytic carbon.[36]

This paper describes a detailed chemical kinetic model that simulates the gas-phase reactions in CVD of carbon from unsaturated light hydrocarbons. To validate this model, we used the experimental results from our previous analysis,[37] in which we identified and quantified more than 40 gas-phase species in the CVD of carbon from ethylene, acetylene, and propylene. The computed and experimental mole fractions were compared for more than 30 products, including hydrogen and hydrocarbons ranging from methane to coronene. Reaction rate and sensitivity analyses were also conducted to determine the dominant reaction route and crucial steps in the mechanism.

2. Methods

2.1. Experimental Data. The experimental procedure and database used to validate the mechanism have been described in our previous work.[37] A vertical flow reactor was used and operated at 900 °C, at a total pressure of 2−15 kPa and residence times up to 1.6 s. No inert diluent gas was used; in other words, the pressure means the initial concentration of the precursor. A 4-cm-long isothermal zone was located at the center of the reactor (total length of 44 cm), into which a honeycomb monolith made of cordierite with 400 channels per square inch was placed. Ethylene, acetylene, and propylene (purchased from Air Liquide) were used as the source hydrocarbons. Reaction products were analyzed using both on-line and off-line gas chromatography. The estimated uncertainties in determining the concentrations of gaseous, major condensing products, and minor condensing products (mainly PAHs) were ±9%, ±28%, and ±32%, respectively.

2.2. Mechanism. We developed a gas-phase reaction mechanism by compiling elementary reactions reported in the literature. This reaction mechanism consists of 227 species and 827 elementary reactions, 798 of which are reversible. The mechanism, the references for each of the elementary reactions, the thermodynamic data for all species, and the species abbreviations and corresponding chemical formulas are given in the Supporting Information and can also be downloaded from www.detchem.com.

Mechanism compilation began with extraction of hydrocarbon parts (non-oxygen-containing reactions and species) from the mechanism of aromatics formation in acetylene and ethylene flames reported by Wang and Frenklach,[38] which was later extended by Appel et al.[39] This mechanism is very comprehensive and covers the formation of PAHs up to pyrene, but it does not include the formation of hydrocarbons with odd numbers of carbon atoms, such as toluene and indene, and it does not distinguish the substituted positions of the PAHs. The former were obtained from the mechanism proposed by Marinov et al.,[40] who used many reactions including C_5, C_7, and C_9 species. The detailed reactions for C_3 and C_4 species were added from the mechanism reported by Hidaka and co-workers[16,41] and Tsang.[42] The very detailed mechanism of the PAHs up to coronene, from Richter et al.,[43] who also distinguished the substituted positions of the PAHs, was added to extend the model performance and was ultimately the largest contributor to our mechanism. Several reactions that involved acetone pyrolysis[44,45] were included, because a significant amount of acetone was present in the acetylene cylinder used in the experiments. Thermochemical data (NASA polynomial form) were taken from several sources.[38,43,46]

Table 1. Properties of the Source Gases and the Initial Compositions Used in the Computations

source hydrocarbon	purity (vol %)[a]	composition used in the computation (mole fraction)
ethylene	>99.4	0.994 C_2H_4, 0.002 CH_4, 0.004 C_2H_6
acetylene	>99.6	0.980 C_2H_2, 0.002 CH_4, 0.018 acetone
propylene	>99.5	0.996 C_3H_6, 0.001 CH_4, 0.003 C_3H_8

[a] Company-reported values.

2.3. Computation. Simulations were conducted using the HOMREA software package that was designed for computational analysis of time-dependent homogeneous reaction systems.[47] In this program, the input includes the forward reaction-rate parameters and thermodynamic polynomials for all of the participating species, in addition to temperature, pressure, and reactant concentrations. The program calculates the rate constant of the backward reaction for every given reversible reaction.

Computations were performed under isobaric and isothermal conditions. The temperature profile along the reactor length was not considered in detail, because its inclusion would have resulted in a large computational expense and made the development of the mechanism accompanying the numerous iterative comparisons of the computational outputs with the experimental data laborious. The calculations using the present mechanism and the software DETCHEM^{PLUG},[48] which incorporates the axial temperature profiles of the reactor, show almost the same outputs as the HOMREA results; therefore, pre-reactions/post-reactions before/beyond the hot zone can be neglected. The purities of the source hydrocarbons and the initial compositions used in the computations are summarized in Table 1. The compositions of the source hydrocarbons were based on the values reported by the manufacturer, with the exception of acetylene, which was analyzed by gas chromatography coupled with mass spectroscopy (GC/MS) and was determined to contain 2% (v/v) acetone. Because acetylene is transported and stored dissolved in acetone to prevent explosion, the high fraction of acetone is not surprising. In the computations for acetylene pyrolysis, the initial acetone volume fraction was fixed to 0.018, although the acetone concentration is dependent on the total pressure of acetylene bottle, as discussed by Bergmann et al.[49] Notably, the calculation always led to incorrect predictions if pure (100%) hydrocarbons were used as the input. Small amounts of impurities, such as methane, ethane, and propane, have an important role in initiating the reactions. Although the addition of methane (0.2 vol %) in the acetylene computations was not validated, it was necessary to initiate the reactions for an acetylene feed. Those species predicted by the mechanism to have reasonable profiles were also analyzed for sensitivity and reaction rates, to identify the crucial reaction steps.

3. Comparison of the Model Prediction with Experimental Data for the Major Species and Reaction Rate Analysis

3.1. Ethylene Pyrolysis. The measured and predicted mole fractions of six major compounds (ethylene, hydrogen, acetylene, methane, 1,3-butadiene, and benzene) found in the CVD experiments conducted with an ethylene precursor at 900 °C and 8 kPa are shown in Figure 1. The experimental mole

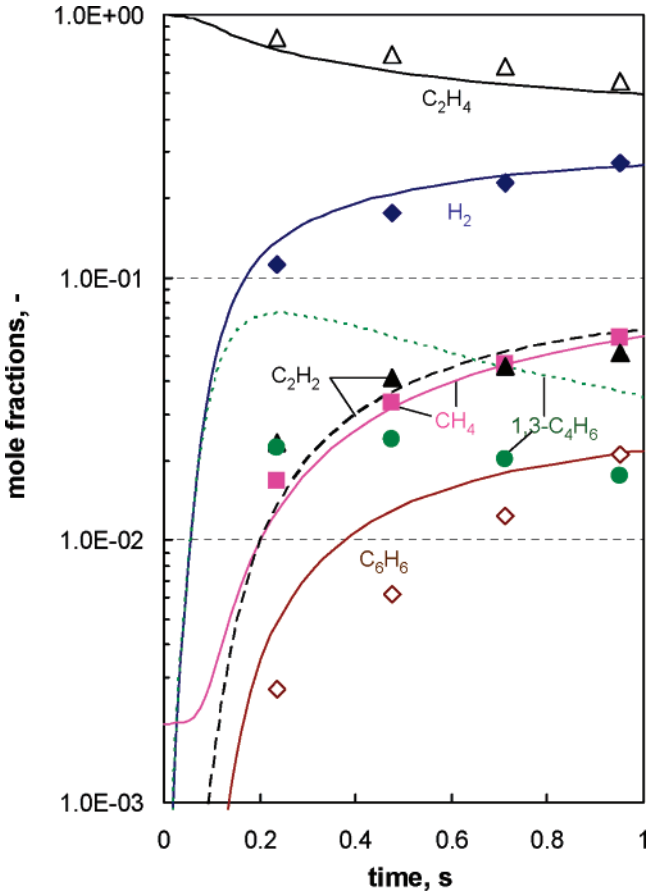

Figure 1. Comparison of model predictions (lines) with experimental mole fraction profiles (symbols) of major species during ethylene pyrolysis in a flow reactor at 900 °C and 8 kPa.

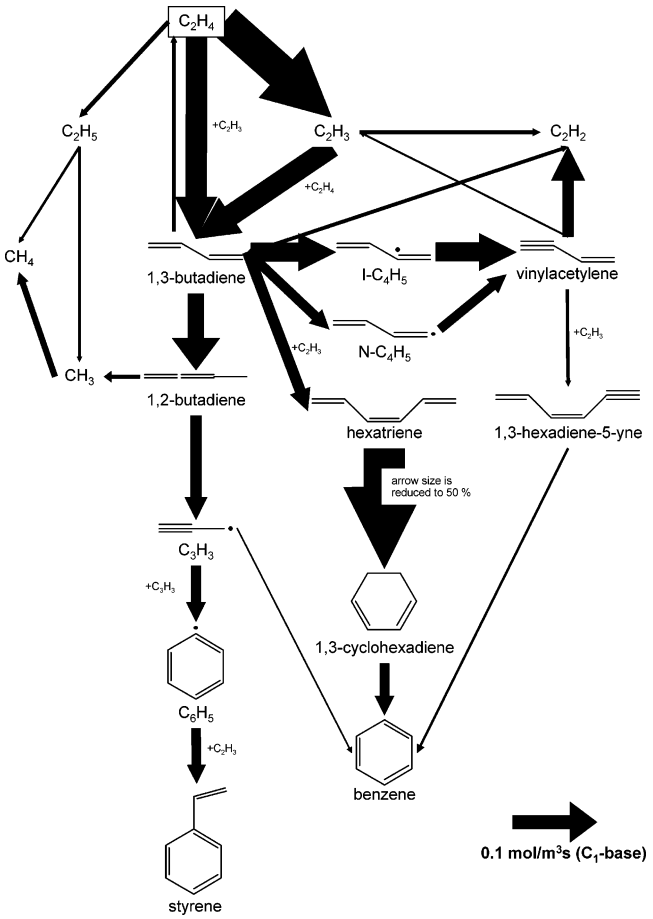

Figure 2. Reaction-rate analysis in ethylene pyrolyisis under conditions of 900 °C, 8 kPa, and 0.5 s. The thickness of the arrow represents the local rates at $\tau = 0.5$ s for the formation or consumption of the species expresses as C_1-base (in units of mol m^{-3} s^{-1}).

fractions are plotted as a function of time, which corresponds to the effective residence time in the isothermal zone in the reactor. (The term "effective residence time" was defined in our previous work.[37]) The model predicts the consumption of ethylene and the formation of hydrogen, acetylene, and methane. The formation of 1,3-butadiene is overpredicted for the entire range of residence time, and benzene is slightly overpredicted for short residence times. Nevertheless, the model qualitatively predicts all of the trends observed experimentally for all species.

The reaction-rate analysis obtained for the major hydrocarbon species in ethylene pyrolysis under conditions of 900 °C, 8 kPa, and 0.5 s is shown in Figure 2. The thickness of the arrows represents the local rate of consumption or formation of the species at 0.5 s. The rates are expressed as C_1-base (in units of mol m^{-3} s^{-1}). Below, we discuss the dominant reactions for the formation or consumption of the major species. Values given below in parentheses denote the contributions of each reaction to the formation or consumption of that species.

Ethylene is consumed by two main reactions, hydrogen abstraction [$C_2H_4 + H \rightarrow C_2H_3 + H_2$ (44%)][38] and vinyl radical addition, which yields 1,3-butadiene [$C_2H_4 + C_2H_3 \rightarrow 1,3\text{-}C_4H_6 + H$ (31%)].[38] Hydrogen addition [$C_2H_4 + H + M \rightarrow C_2H_5 + M$ (6%)][38] and methyl radical attack [$C_2H_4 + CH_3 \rightarrow C_2H_3 + CH_4$ (6%)][38] also contribute to the consumption of ethylene. Acetylene is formed primarily by vinylacetylene decomposition [$C_4H_4 \rightarrow 2C_2H_2$ (40%)][50] and secondarily by $C_2H_3 + M \rightarrow C_2H_2 + H + M$ (16%),[38] $1,3\text{-}C_4H_6 \rightarrow C_2H_4 + C_2H_2$ (13%),[41] and $C_4H_4 + H \rightarrow C_2H_3 + C_2H_2$ (7%).[51]

The main source of methane is the methyl radical, which reacts with hydrogen, ethylene, and 1,3-butadiene to form methane, i.e., $CH_3 + H_2 \rightarrow CH_4 + H$ (31%),[38] $C_2H_4 + CH_3 \rightarrow C_2H_3 + CH_4$ (25%),[38] $1,3\text{-}C_4H_6 + CH_3 \rightarrow N\text{-}C_4H_5 + CH_4$ (9%),[52] and $1,3\text{-}C_4H_6 + CH_3 \rightarrow I\text{-}C_4H_5 + CH_4$ (5%).[52] Ethyl radical decomposition [$C_2H_5 + H_2 \rightarrow CH_4 + CH_3$ (25%)][53] also contributes to methane formation. The primary and secondary sources of methyl radicals are the decomposition of 1,2-butadiene [$1,2\text{-}C_4H_6 + M \rightarrow C_3H_3 + CH_3 + M$ (50%)][38] and ethyl radical decomposition [$C_2H_5 + H_2 \rightarrow CH_4 + CH_3$ (28%)].[53]

The mole-fraction profiles of 1,3-butadiene in both the experiments and model predictions are maximal at ~0.1 s, when the formation and consumption rates are in competition. The subsequent decrease in mole fractions shows that consumption becomes dominant. 1,3-Butadiene is formed almost solely by the reaction $C_2H_4 + C_2H_3 \rightarrow 1,3\text{-}C_4H_6 + H$ (94%),[38] whereas it is consumed by various reactions, primarily isomerization to 1,2-butadiene [$1,3\text{-}C_4H_6 \rightarrow 1,2\text{-}C_4H_6$ (22%)],[54] hydrogen abstraction by radical attack [$1,3\text{-}C_4H_6 + H \rightarrow I\text{-}C_4H_5 + H_2$ (18%),[38] $1,3\text{-}C_4H_6 + H \rightarrow N\text{-}C_4H_5 + Hy$ (9%),[38] and $1,3\text{-}C_4H_6 + C_2H_3 \rightarrow I\text{-}C_4H_5 + C_2H_4$ (8%)],[38] vinyl addition forming hexatriene [$1,3\text{-}C_4H_6 + C_2H_3 \rightarrow L\text{-}C_6H_8 + H$ (9%)],[55] and decomposition [$1,3\text{-}C_4H_6 \rightarrow C_2H_4 + C_2H_2$ (9%)].[41]

Benzene is formed primarily from 1,3-cyclohexadiene [$1,3\text{-}C_6H_8 \rightarrow C_6H_6 + H_2$ (52%)][56] and secondarily by cyclization of 1,3-hexadiene-5-yne [$L\text{-}C_6H_6 + H \rightarrow C_6H_6 + H$ (11%)].[51] Toluene decomposition [$C_7H_8 + H \rightarrow C_6H_6 + CH_3$ (7%)][57] and hydrogen removal from 1,3-cyclohexadienyl [$C\text{-}C_6H_7 \rightarrow C_6H_6 + H$ (6%)][58] also produce benzene. Most of the benzene comes from C_6 species. The direct formation of benzene from

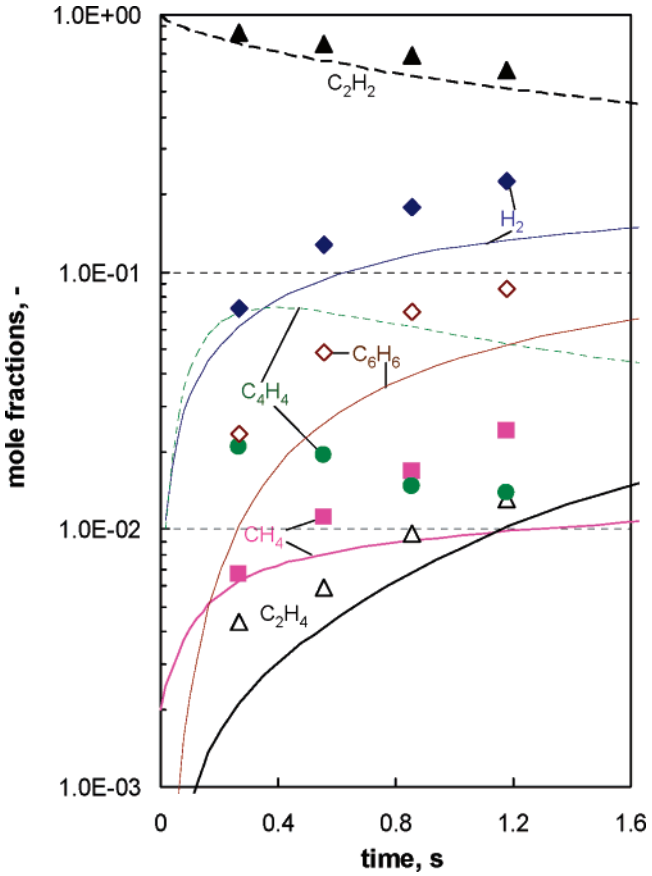

Figure 3. Comparison of model predictions (lines) with experimental mole fraction profiles (symbols) of minor species during acetylene pyrolysis in a flow reactor at 900 °C and 8 kPa.

combinations of C_3 species and combinations of C_4 and C_2 species (such as $AC_3H_5 + C_3H_3 \rightarrow C_6H_6 + 2H$ (4%),[27] $AC_3H_4 + C_3H_3 \rightarrow C_6H_6 + H$ (3%),[59] and $N-C_4H_5 + C_2H_2 \rightarrow C_6H_6 + H$ (3%)[51]) are minor. 1,3-Cyclohexadiene, which is a major benzene precursor, is produced by the very rapid isomerization of hexatriene, which is predominantly (99%) produced via the reaction $1,3\text{-}C_4H_6 + C_2H_3 \rightarrow L\text{-}C_6H_8 + H$.[55] The other precursor, 1,3-hexadiene-5-yne, is produced by $C_4H_4 + C_2H_3 \rightarrow L\text{-}C_6H_6 + H$ (99%).[38] $N\text{-}C_4H_5$ and $I\text{-}C_4H_5$, which was formed by hydrogen removal from 1,3-butadiene by radical (H or CH_3) attack, are the main precursors of vinylacetylene (C_4H_4).

3.2. Acetylene Pyrolysis. The measured and predicted mole fractions of the six major compounds observed in the CVD experiments using acetylene as a precursor are shown in Figure 3; these compounds were acetylene, hydrogen, benzene, vinylacetylene, methane, and ethylene. The consumption of acetylene was well-predicted, and product formation was predicted fairly well, although vinylacetylene was significantly overpredicted. Again, the simulation qualitatively predicted all of the trends observed experimentally.

Figure 4 shows the result of the reaction-rate analysis obtained according to the proposed mechanism for major hydrocarbon species in acetylene pyrolysis under conditions of 900 °C, 8 kPa, and 0.5 s. The chemistry of acetylene pyrolysis is simpler than ethylene and propylene pyrolysis. Acetylene is consumed primarily by dimerization to form vinylacetylene ($2C_2H_2 \rightarrow C_4H_4$ (68%))[50] and secondarily by diacetylene formation ($2C_2H_2 \rightarrow C_4H_2 + H_2$ (17%)).[60] Combination of acetylene and vinylacetylene, $C_4H_4 + C_2H_2 \rightarrow$ benzene,[61] contributes to 7% of acetylene consumption but the 95% of benzene formation. Ninety-eight percent of vinylacetylene is formed by $2C_2H_2 \rightarrow C_4H_4$.[50]

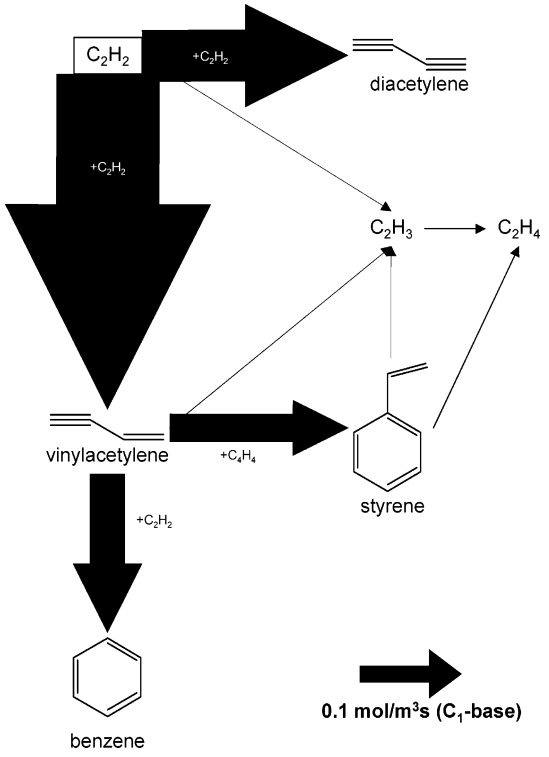

Figure 4. Reaction-rate analysis in acetylene pyrolysis under conditions of 900 °C, 8 kPa, and 0.5 s. The thickness of the arrow represents the local rates at $\tau = 0.5$ s for the formation or consumption of the species expresses as C_1-base (in units of mol m^{-3} s^{-1}).

Ethylene is primarily formed by the decomposition of styrene, styrene + H → $C_6H_5 + C_2H_4$ (51%).[62] The second source of ethylene is the reaction of vinyl radical with hydrogen (27%).[38] The decomposition of 1,3-butadiene, $1,3\text{-}C_4H_6 + H \rightarrow C_2H_4 + C_2H_3$ (8%),[38] also contributes to the ethylene formation.

Methane is formed predominantly from methyl radicals that abstract the H radical from other molecules via reactions such as $CH_3 + H_2 \rightarrow CH_4 + H$ (76%).[38] Sixty-four percent of methyl is yielded from acetone, which is a contamination (2 vol %) in the acetylene cylinder. The reaction paths are acetone → $CH_3CO + CH_3$ (32%)[45] and $CH_3CO \rightarrow CH_3 + CO$ (32%).[44] The decompositions of 1-butyne and 1,2-butadiene, such as 1-butyne → $C_3H_3 + CH_3$ (14%)[41] and $1,2\text{-}C_4H_6 + M \rightarrow C_3H_3 + CH_3 + M$ (10%),[38] also produce methyl radicals.

3.3. Propylene Pyrolysis. The nine major compounds (propylene, methane, ethylene, hydrogen, benzene, acetylene, propyne, propadiene, and 1,3-butadiene) observed in the CVD experiments using propylene as a precursor are shown in Figure 5. The propylene mole fraction is markedly overpredicted at residence times of <0.5 s and is underpredicted at longer residence times. The methane and ethylene profiles are in excellent agreement, and the formation of the other products is predicted fairly well. The prediction curves also capture the experimental trends well, except for those of acetylene and 1,3-butadiene.

Figure 6 shows the result of the reaction-rate analysis obtained according to the proposed mechanism for major hydrocarbon species in propylene pyrolysis under conditions of 900 °C, 8 kPa, and 0.5 s. The chemistry of propylene pyrolysis is most complex. Propylene is consumed primarily by the decomposition that yields methyl and ethylene: $C_3H_6 + H \rightarrow C_2H_4 + CH_3$ (32%).[16] Radical attacks such as $C_3H_6 + C_5H_5 \rightarrow AC_3H_5 + C_5H_6$ (28%),[63] $C_3H_6 + H \rightarrow AC_3H_5 + H_2$ (14%),[64] and $C_3H_6 + CH_3 \rightarrow AC_3H_5 + CH_4$ (6%)[42] convert propylene into AC_3H_5 (allyl radical, $CH_2{=}CHCH_2\cdot$). Hydrogen addition (C_3H_6 + H

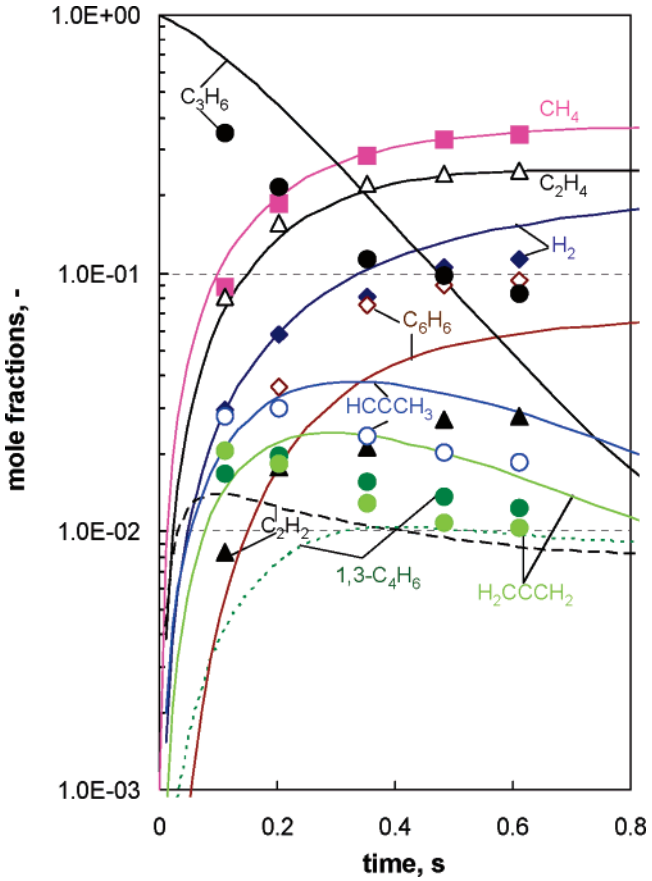

Figure 5. Comparison of model predictions (lines) with experimental mole fraction profiles (symbols) of major species during propylene pyrolysis in a flow reactor at 900 °C and 8 kPa.

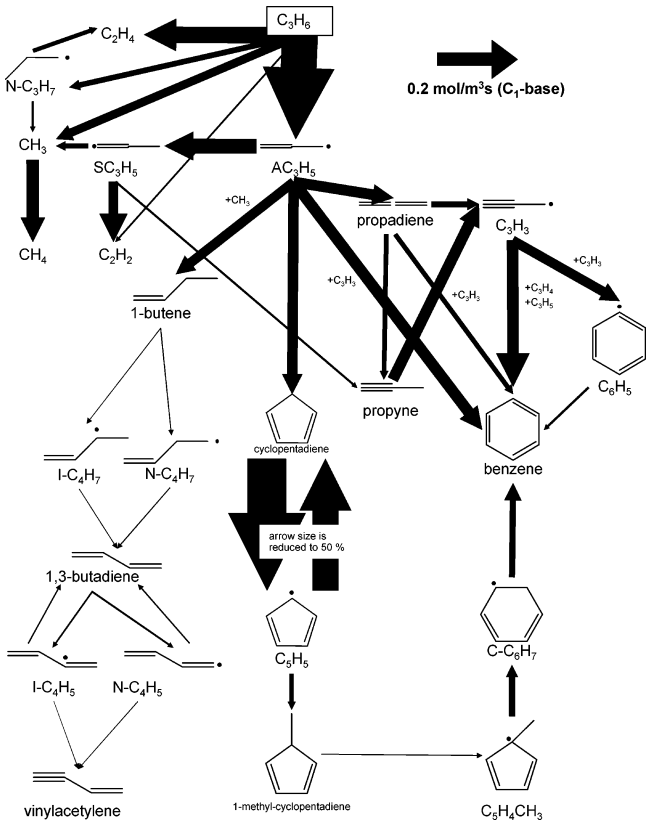

Figure 6. Reaction rate analysis in propylene pyrolysis under conditions of 900 °C, 8 kPa, and 0.5 s. The thickness of the arrow represents the local rates at $\tau = 0.5$ s for the formation or consumption of the species expresses as C_1-base (in units of mol m^{-3} s^{-1}).

→ N-C_3H_7 (7%))[65] and decomposition ($C_3H_6 \rightarrow C_2H_2 + CH_4$ (3%))[16] also consume propylene.

More than 80% of methane is formed through methyl radicals. The direct formation of methane, via $C_3H_6 \rightarrow C_2H_2 + CH_4$,[16] contributes to only 5% of methane formation. Methyl radicals are primarily formed by $C_3H_6 + H \rightarrow C_2H_4 + CH_3$ (50%).[16] The decompositions of SC_3H_5 (2-methyl vinyl radical, ·HC=CHCH$_3$) and N-C_3H_7 (CH$_3$CH$_2$CH$_2$·), such as $SC_3H_5 \rightarrow C_2H_2 + CH_3$ (29%)[65] and N-$C_3H_7 \rightarrow C_2H_4 + CH_3$ (12%),[66] also yield methyl radicals. SC_3H_5 is predominantly produced via the isomerization of allyl radicals.[67]

Ethylene is formed directly by $C_3H_6 + H \rightarrow C_2H_4 + CH_3$ (56%)[16] and N-$C_3H_7 \rightarrow C_2H_4 + CH_3$ (13%).[66] There is an indirect route through vinyl radicals, $C_2H_3 + C_5H_6 \rightarrow C_2H_4 + C_5H_5$ (25%).[57]

Combinations between C_3 species such as $AC_3H_5 + C_3H_3 \rightarrow C_6H_6 + 2H$ (40%)[26] and $AC_3H_4 + C_3H_3 \rightarrow C_6H_6 + H$ (26%)[59] are major routes to benzene. There are also two other pathways to benzene through C−C_6H_7 (C−$C_6H_7 \rightarrow C_6H_6 + H$ (17%)[58]) and phenyl radical ($C_6H_5 + AC_3H_4 \rightarrow C_6H_6 + C_3H_3$ (6%)[26]). Isomerization of 1-methylcyclopentadiene is a predominant source of C−C_6H_7. Recombination of propargyls ($C_3H_3 + C_3H_3 \rightarrow C_6H_5 + H$)[40] is the primary source of phenyl.

Propyne is formed primarily by isomerization of propadiene ($AC_3H_4 \rightarrow PC_3H_4$ (63%))[59] and secondarily by decomposition ($SC_3H_5 \rightarrow PC_3H_4 + H$ (25%)[68]). Propadiene is formed predominantly by $AC_3H_5 + C_5H_5 \rightarrow AC_3H_4 + C_5H_6$ (86%).[13]

Acetylene is yielded primarily by $SC_3H_5 \rightarrow C_2H_2 + CH_3$ (70%)[65] and secondarily by $C_3H_6 \rightarrow C_2H_2 + CH_4$ (11%).[16] Various routes are found in 1,3-butadiene formation. Forty-seven percent of 1,3-C_4H_6 is formed from hydrogen abstraction of C_4H_5 radicals (N-C_4H_5 and I-C_4H_5). Another major route is the decomposition of C_4H_7 radicals (I-C_4H_7 and N-C_4H_7), which accounts for 28% of 1,3-butadiene formation. Metathesis of two olefins such as $C_3H_6 + C_2H_3 \rightarrow$ 1,3-$C_4H_6 + CH_3$ (19%)[42] also contributes to the formation of 1,3-butadiene.

4. Sensitivity Analysis

The time-dependent changes in the relative sensitivity coefficients computed for the three major species of interest in the pyrolysis of ethylene (upper), acetylene (middle), and propylene (bottom), under conditions of 900 °C and 8 kPa, are shown in Figure 7. The sensitivity coefficients were calculated for each source hydrocarbon, benzene, and important intermediates, such as 1,3-butadiene, vinylacetylene, and propyne for the pyrolyses of ethylene, acetylene, and propylene, respectively. A positive sensitivity coefficient indicates that the reaction enhances the species production rate or slows its consumption rate, whereas a negative sensitivity coefficient indicates the opposite effect. Although our mechanism consists of more than 800 reactions, the reactions that significantly affect the formation or consumption of the species of interest are rather limited in number. Only a few sensitive reactions are found for ethylene and acetylene pyrolysis, whereas 16 sensitive reactions are found for propylene pyrolysis.

In ethylene pyrolysis, ethylene consumption is greatly affected by ethylene reactions 7 (reaction E07) (vinyl formation from hydrogen attack of ethylene) and 8 (reaction E08) (vinyl addition to ethylene yielding 1,3-butadiene). These reactions are also sensitive in regard to the formation of 1,3-butadiene, especially at short residence times. Reactions E13 (isomerization of 1,3-butadine to 1,2-butadiene) and E10 (decomposition of 1,2-

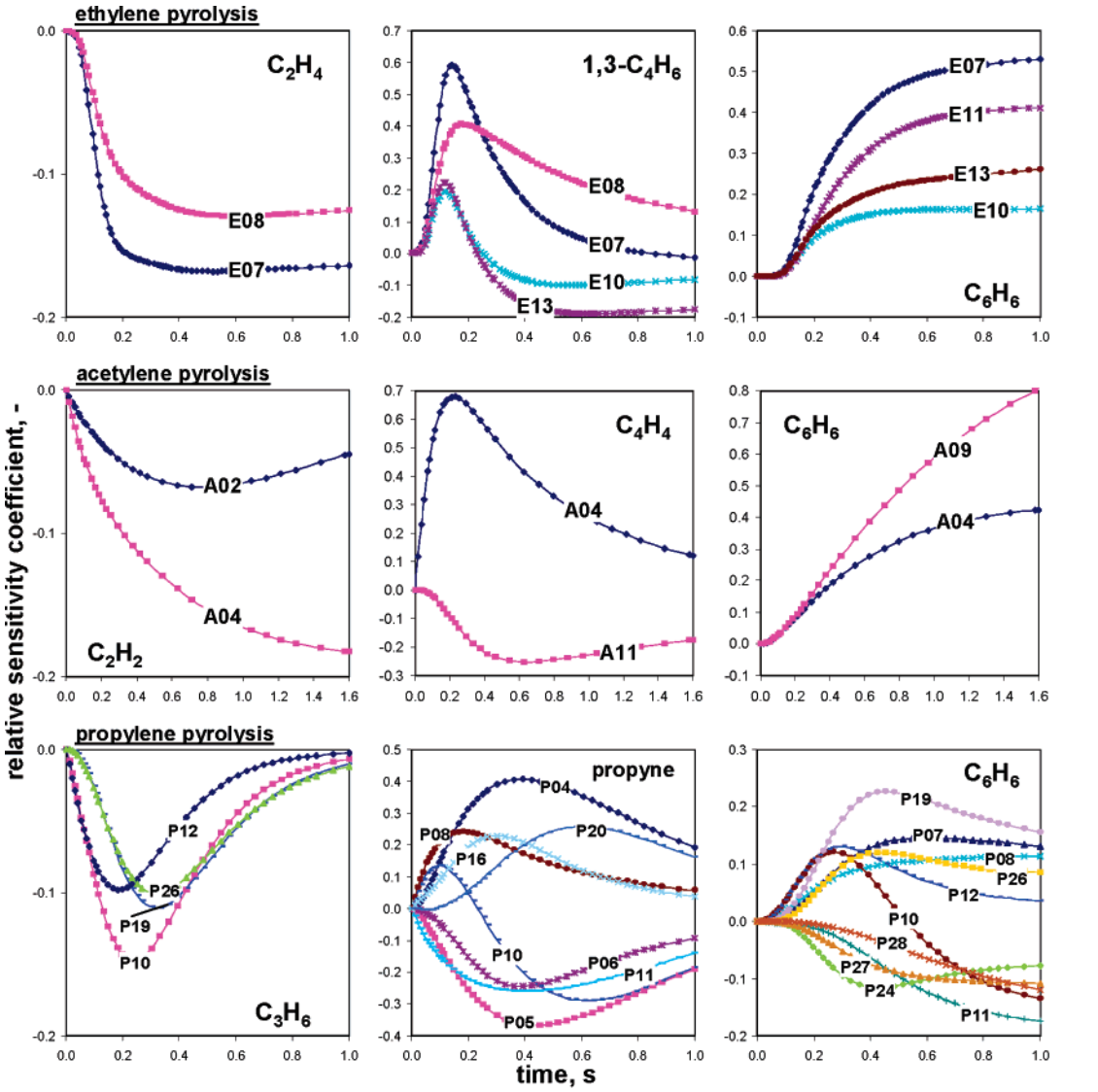


```
ethylene pyrolysis
E07:  C2H4      +H       ->  H2      +C2H3
E08:  C2H4      +C2H3    ->  C4H6    +H
E10:  C4H612    +M(2)    ->  CH3     +C3H3
E11:  C4H6      +C2H3    ->  H       +L-C6H8
E13:  C4H6               ->  C4H612

acetylene pyrolysis
A02:  C2H2      +C2H2    ->  H2      +C4H2
A04:  C2H2      +C2H2    ->  C4H4
A09:  C2H2      +C4H4    ->  C6H6
A11:  C4H4      +C4H4    ->  C8H8

propylene pyrolysis
P04:  AC3H4             ->  PC3H4
P05:  PC3H4             ->  AC3H4
P06:  PC3H4     +CH3    ->  CH4     +C3H3
P07:  C3H3      +AC3H5  ->  C6H6    +H        +H
P08:  SC3H5             ->  PC3H4   +H
P10:  AC3H5             ->  SC3H5
P11:  SC3H5             ->  C2H2    +CH3
P12:  C3H6              ->  H       +AC3H5
P16:  C3H6      +CH3    ->  CH4     +AC3H5
P19:  C5H6              ->  H       +C5H5
P20:  AC3H5     +C5H5   ->  AC3H4   +C5H6
P24:  C2H3      +C5H6   ->  C2H4    +C5H5
P25:  AC3H5     +C5H6   ->  C3H6    +C5H5
P26:  C3H6      +C5H5   ->  AC3H5   +C5H6
P27:  C2H2      +C5H5   ->  C7H7
P28:  C6H6      +C7H7   ->  H       +BENZYLB
```

Figure 7. Relative sensitivity coefficients versus time computed for three major species of interest in pyrolysis of ethylene (upper), acetylene (middle), and propylene (bottom) at 900 °C and 8 kPa.

butadiene) are sensitive in regard to 1,3-butadiene consumption at longer residence times. Benzene formation is affected greatly by reactions E07, E10, and E13, as well as by reaction E11 (vinyl addition to 1,3-butadiene yielding hexatriene).

Acetylene pyrolysis is rather simple. Acetylene consumption is greatly affected by acetylene reactions 2 (reaction A02) (combination of acetylene to form diacetylene) and 4 (reaction A04) (combination of acetylene to form vinylacetylene). Reaction A04 is also sensitive in regard to vinylacetylene formation, especially at short residence times. Reaction A11 (the combination of vinylacetylene to form cyclo-octatetracene) is sensitive in regard to vinylacetylene consumption. Benzene formation is affected greatly by reactions A04 and A09 (acetylene addition to vinylacetylene, yielding benzene).

Several sensitive reactions were found for propylene pyrolysis. Propylene consumption is greatly affected by propylene reactions 10 (reaction P10) (isomerization of allyl to 2-methyl vinyl radical), 19 (reaction P19) (cyclopentadiene decomposition yielding cyclopentadienyl radical), 26 (reaction P26) (allyl formation from cyclopentadienyl radical attack), and 12 (reaction P12) (decomposition of propylene to form allyl). The cyclopentadienyl radical is likely a key species in propylene pyrolysis.

Table 2. Rate Constant Parameters for the Selected Reactions That Exhibit Global Sensitivity Coefficients of >0.2 (Mole Fractions of $>10^{-2}$) for the Formation and Consumption of Major Compounds in the Pyrolysis of Ethylene, Acetylene, and Propylene[a]

reaction[b]	A	n	E_a	k at 900 °C
1. $H_2 + CH_3 \rightarrow CH_4 + H$	2.31×10^7	1.62	41.54	3.06×10^{10}
2. $H + C_2H_5 \rightarrow CH_4 + CH_3$	3.49×10^{12}	0.00	46.16	3.07×10^{10}
3. $C_2H_3 + M \rightarrow C_2H_2 + H + M$	reverse Troe falloff reaction			4.05×10^{3}[c]
4. $C_2H_2 + C_2H_2 \rightarrow H_2 +$ diacetylene	1.50×10^{13}	0.00	178.67	1.66×10^5
5. $C_2H_2 + C_2H_2 \rightarrow$ vinylacetylene	5.50×10^{12}	0.00	154.65	7.4×10^5
6. vinylacetylene $\rightarrow C_2H_2 + C_2H_2$	8.65×10^{13}	0.00	312.85	1.01×10^0
7. $C_2H_2 + C_2H_3 \rightarrow$ vinylacetylene + H	4.60×10^{16}	−1.25	35.15	1.82×10^{11}
8. vinylacetylene + H $\rightarrow C_2H_2 + C_2H_3$	3.93×10^{17}	−1.25	31.09	2.36×10^{12}
9. $C_2H_4 + H + M \rightarrow C_2H_5 + M$	Troe falloff reaction			1.21×10^{5}[c]
10. $C_2H_5 + M \rightarrow C_2H_4 + H + M$	reverse Troe falloff reaction			1.15×10^{4}[c]
11. $C_2H_4 + H \rightarrow H_2 + C_2H_3$	1.33×10^6	2.53	51.21	4.06×10^{11}
12. $H_2 + C_2H_3 \rightarrow C_2H_4 + H$	7.41×10^4	2.53	38.28	8.52×10^{10}
13. $C_2H_4 + CH_3 \rightarrow CH_4 + C_2H_3$	2.27×10^5	2.00	39.49	6.03×10^9
14. $C_2H_4 + C_2H_3 \rightarrow$ 1,3-butadine + H	7.40×10^{14}	−0.66	35.23	1.88×10^{11}
15. 1,3-butadine + H $\rightarrow C_2H_4 + C_2H_3$	2.77×10^{16}	−0.66	30.91	1.10×10^{13}
16. $H + C_2H_6 \rightarrow H_2 + C_2H_5$	1.15×10^8	1.90	31.51	3.08×10^{12}
17. $C_2H_4 + C_2H_5 \rightarrow C_2H_3 + C_2H_6$	5.60×10^{12}	0.00	75.51	2.43×10^9
18. 1,2-butadine + M $\rightarrow CH_3 + C_3H_3 + M$	reverse Troe falloff reaction			1.48×10^{2}[c]
19. $C_3H_3 + C_3H_3 \rightarrow H + C_6H_5$	3.00×10^{12}	0.00	0.00	3.00×10^{12}
20. propadiene $\rightarrow$ propyne	2.50×10^{12}	0.00	246.87	2.54×10^1
21. propyne $\rightarrow$ propadiene	1.58×10^{12}	0.00	248.16	1.40×10^1
22. propadiene + $CH_3 \rightarrow CH_4 + C_3H_3$	1.00×10^{12}	0.00	33.47	3.23×10^{10}
23. propyne + H $\rightarrow H_2 + C_3H_3$	1.15×10^8	1.90	31.51	3.08×10^{12}
24. propyne + $CH_3 \rightarrow CH_4 + C_3H_3$	1.00×10^{12}	0.00	33.47	3.23×10^{10}
25. $C_3H_3 + CH_2{=}CHCH_2{\cdot} \rightarrow C_6H_6 + H + H$	5.60×10^{20}	−2.54	7.10	4.33×10^{12}
26. $\cdot CH{=}CHCH_3 \rightarrow$ propyne + H	1.40×10^{13}	0.00	146.30	4.28×10^6
27. $\cdot CH{=}CHCH_3 \rightarrow CH_2{=}CHCH_2{\cdot}$	5.00×10^{13}	0.00	154.70	6.45×10^6
28. $CH_2{=}CHCH_2{\cdot} \rightarrow \cdot CH{=}CHCH_3$	7.67×10^{13}	0.00	242.46	1.22×10^3
29. $\cdot CH{=}CHCH_3 \rightarrow C_2H_2 + CH_3$	1.30×10^{13}	0.00	139.75	7.77×10^6
30. $C_2H_2 + CH_3 \rightarrow \cdot CH{=}CHCH_3$	3.32×10^{11}	0.00	34.17	9.99×10^9
31. $C_3H_6 \rightarrow H + CH_2{=}CHCH_2{\cdot}$	4.39×10^{15}	0.00	367.97	1.80×10^{-1}
32. $C_3H_6 \rightarrow CH_4 + C_2H_2$	1.80×10^{12}	0.00	292.70	1.66×10^{-1}
33. $C_3H_6 + H \rightarrow C_2H_4 + CH_3$	3.40×10^{13}	0.00	14.64	7.58×10^{12}
34. $C_3H_6 + H \rightarrow H_2 + CH_2{=}CHCH_2{\cdot}$	6.00×10^{12}	0.00	6.28	3.15×10^{12}
35. $C_3H_6 + CH_3 \rightarrow CH_4 + CH_2{=}CHCH_2{\cdot}$	2.21×10^0	3.50	23.75	1.07×10^{10}
36. $C_3H_6 + H \rightarrow CH_3CH_2CH_2{\cdot}$	1.85×10^{13}	0.00	23.08	1.74×10^{12}
37. $CH_2{=}CHC{\cdot}{=}CH_2 \rightarrow$ vinylacetylene + H	1.74×10^{53}	−12.44	245.20	1.38×10^4
38. 2-vinylacetylene $\rightarrow$ styrene	7.50×10^{13}	0.00	159.00	6.23×10^6
39. 2-vinylacetylene $\rightarrow$ cyclooctatetracene	4.37×10^{10}	0.00	76.99	1.63×10^7
40. $C_2H_2 +$ vinylacetylene $\rightarrow C_6H_6$	4.47×10^{11}	0.00	126.00	1.09×10^6
41. 1,3-butadine $\rightarrow C_2H_2 + C_2H_4$	6.40×10^{13}	0.00	322.60	2.75×10^{-1}
42. 1,3-butadine + H $\rightarrow H_2 + CH_2{=}CHC{\cdot}{=}CH_2$	6.65×10^5	2.53	38.66	7.35×10^{11}
43. 1,3-butadine + $C_2H_3 \rightarrow$ H + hexatriene	1.00×10^{10}	1.05	58.50	4.15×10^{10}
44. 1,2-butadine $\rightarrow$ 1,3-butadine	2.50×10^{13}	0.00	263.60	4.56×10^1
45. 1,3-butadine $\rightarrow$ 1,2-butadine	1.17×10^{14}	0.00	317.11	8.84×10^{-1}
46. 1-butene $\rightarrow CH_3 + CH_2{=}CHCH_2{\cdot}$	1.10×10^{16}	0.00	325.08	3.67×10^1
47. $CH_3 + CH_2{=}CHCH_2{\cdot} \rightarrow$ 1-butene	4.76×10^{13}	0.00	16.18	9.06×10^{12}
48. H + CYPD$\cdot \rightarrow$ CYPD	2.00×10^{14}	0.00	0.00	2.00×10^{14}
49. CYPD $\rightarrow$ H + CYPD$\cdot$	1.21×10^{15}	0.00	321.13	6.05×10^0
50. CH_3 + CYPD$\cdot \rightarrow CH_3$CYPD	1.00×10^{-1}	0.00	0.00	1.00×10^{13}
51. CH_3CYPD $\rightarrow CH_3$ + CYPD$\cdot$	2.38×10^{15}	0.00	282.05	6.55×10^2
52. $CH_2{=}CHCH_2{\cdot}$ + CYPD$\cdot \rightarrow$ propadiene + CYPD	1.00×10^{12}	0.00	0.00	1.00×10^{12}
53. propadiene + CYPD $\rightarrow CH_2{=}CHCH_2{\cdot}$ + CYPD$\cdot$	4.28×10^{12}	0.00	94.17	2.74×10^8
54. H + CYPD $\rightarrow H_2 +$ CYPD$\cdot$	2.19×10^8	1.77	12.55	1.64×10^{13}
55. $C_2H_2 + CH_2{=}CHCH_2{\cdot} \rightarrow$ H + CYPD	3.26×10^{11}	0.00	15.85	6.42×10^{10}
56. C_2H_3 + CYPD $\rightarrow C_2H_4 +$ CYPD$\cdot$	6.00×10^{12}	0.00	0.00	6.00×10^{12}
57. $CH_2{=}CHCH_2{\cdot}$ + CYPD $\rightarrow C_3H_6 +$ CYPD$\cdot$	2.00×10^{-1}	4.00	0.00	3.79×10^{11}
58. C_3H_6 + CYPD$\cdot \rightarrow CH_2{=}CHCH_2{\cdot}$ + CYPD	7.27×10^{-1}	4.00	46.85	1.13×10^{10}
59. styrene + H $\rightarrow C_2H_4 + C_6H_5$	1.31×10^{14}	0.00	37.94	2.68×10^{12}
60. CH_3CYPD $\rightarrow$ H + CH_3CYPD$\cdot$	3.48×10^{15}	0.00	327.09	9.45×10^0
61. CH_3 + CYPD$\cdot \rightarrow$ H + CH_3CYPD$\cdot$	1.46×10^{13}	0.00	45.04	1.44×10^{11}
62. C_2H_2 + CYPD$\cdot \rightarrow$ benzyl	4.96×10^{11}	0.00	43.25	5.88×10^9
63. indene + H $\rightarrow H_2 +$ indenyl	2.19×10^8	1.77	12.55	1.64×10^{13}

[a] Conditions: 900 °C, 8 kPa, and $\tau = 0.5$ s, where $k = AT^n \exp[-E_a/(RT)]$. [b] CYPD = cyclopentadiene; CYPD$\cdot$ = cyclopentadienyl. [c] Values are for a pressure of 8 kPa.

The rates of formation (reaction P19) and hydrogen abstraction (reaction P26) affect propylene consumption. The isomerization of propadiene to propyne (reaction P04) is the most sensitive reaction for propyne formation, whereas its reverse reaction (reaction P05) is most sensitive for propyne consumption. Reactions P08 (direct formation of propyne from the decomposition of 2-methyl vinyl radical) and P16 (allyl formation from methyl attack on propylene) are sensitive for propyne formation at short residence times, whereas reaction P20 (propadiene formation from allyl by cyclopentadienyl attack) becomes sensitive at longer residence times. The isomerization of allyl to the 2-methyl vinyl radical (reaction P10) initially has a positive effect on propyne formation, but later has a negative effect. Propyne conversion to propargyl by hydrogen abstraction

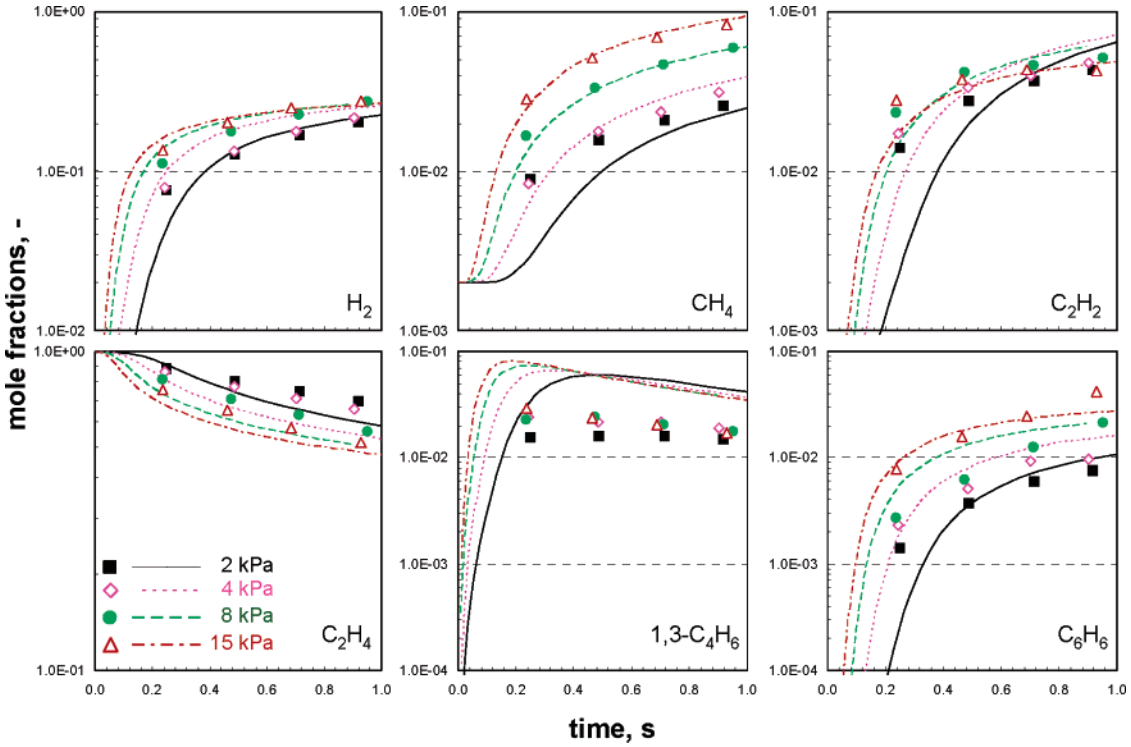

Figure 8. Comparison of model predictions (lines) with experimental mole fraction profiles (symbols) of major species during ethylene pyrolysis in a flow reactor at 900 °C and varying pressures.

by methyl (reaction P06) and the conversion of the 2-methyl vinyl radical into acetylene and methyl (reaction P11) are sensitive in propyne consumption. Benzene formation is affected by reactions P19 and P07 (the combination of propargyl and allyl to form benzene), whereas reactions P08, P12, and P26 have positive effects on benzene formation. Cyclopentadienyl also likely has an important role in benzene formation as a source of 1-methyl-cyclopentadine, which converts benzene (see Figure 6). In addition, the hydrogen abstraction of C3 species, creating important intermediates for benzene formation, such as allyl, propadiene, propyne, and propargyl, are also important. Table 2 lists rate constant parameters for the selected reactions that exhibit global sensitivity coefficients of >0.2 for formation and consumption of major compounds (mole fractions larger than 10^{-2}) in the pyrolysis of ethylene, acetylene, and propylene under the conditions of 900 °C, 8 kPa, and $\tau = 0.5$ s.

5. Pressure Dependence

The predictive performance of our mechanism for ethylene pyrolysis at varying pressures (initial concentrations of the precursor hydrocarbons) is shown in Figure 8. Similar figures for the other two source hydrocarbons (acetylene and propylene) are given in the Supporting Information. Generally, the pressure effect on the consumption of the source hydrocarbons, as well as on formation of the major products, is modeled very well. Although some noticeable disagreements between the experimental and computational results are present (e.g., 1,3-butadiene in ethylene pyrolysis), our kinetic model adequately captures the trends of the pressure effect; an increase in pressure enhances consumption of source hydrocarbons and also enhances product formation. However, this simple rule is not valid for acetylene formation in ethylene pyrolysis. The acetylene mole fraction increases with pressure at residence times up to 0.2 s, whereas it is maximal at 8 kPa at longer residence times. Acetylene consumption becomes dominant at the highest pressure tested (15 kPa). This rather complicated trend, which has been observed experimentally, is traced correctly by the computational results.

6. Comparison of the Model Prediction with Experimental Data for the Minor Species

6.1. Minor Species. The mole fractions of minor compounds found in the gas phase for propylene pyrolysis at 900 °C and 8 kPa are shown as a function of residence time in Figure 9. The minor compounds are classified as C_3 and C_4 hydrocarbons (upper), benzene substitutes (middle), and compounds with two rings and acenaphthylene (bottom). Similar figures for the remaining two hydrocarbon sources (ethylene and acetylene) are given in the Supporting Information. Although some gaps in the agreement between the experimental and computational results are noted, especially for acenaphthylene, the mechanism generally predicts the mole fractions of the minor species well, with mole fractions ranging from 10^{-5} to 10^{-2}.

6.2. Polycyclic Aromatic Hydrocarbons (PAHs) Larger than Phenanthrene. The mole fractions of polycyclic aromatic hydrocarbons (PAHs) larger than phenanthrene found in the gas phase from acetylene pyrolysis at 900 °C and 15 kPa are shown as a function of residence time in Figure 10. Similar figures for ethylene and propylene are found in the Supporting Information. The experimental mole fractions of the PAHs range from 10^{-3} to 10^{-5} and generally decrease as the molecular size of the PAHs increases. PAH formation is underpredicted, and the deviations generally become larger as the molecular size of the PAH increases. The computed mole fractions of coronene are 4 orders of magnitude lower than the experimental mole fractions. The experimental uncertainty is ±32%, even for the PAHs formed at low concentration levels. The deviations between the model predictions and experimental data for PAHs larger than pyrene vary from an order of magnitude to several orders of magnitude and are much larger than the experimental uncertainties. This

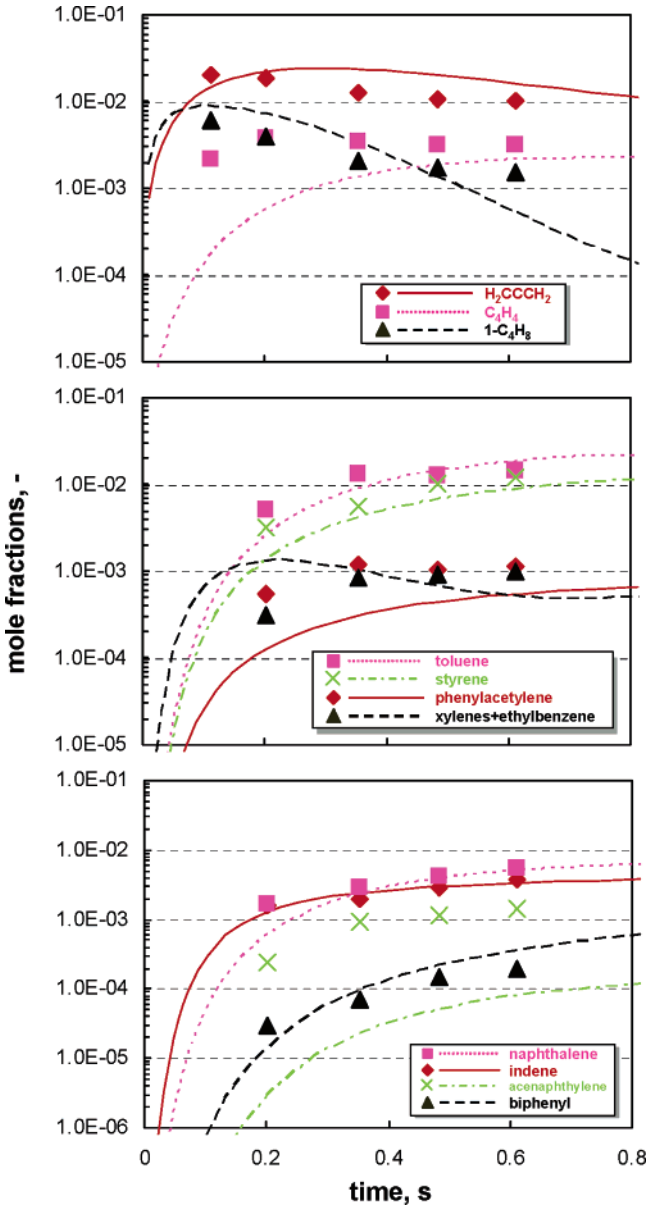

Figure 9. Comparison of model predictions (lines) with experimental mole fraction profiles (symbols) of minor species during propylene pyrolysis in a flow reactor at 900 °C and 8 kPa.

indicates that the experimental uncertainties in determining the concentration of the large PAHs cannot fully explain the gaps between the computations and experiments.

Our model does not satisfactorily predict many PAHs. Our computations are based on simple chemical reactions in a completely mixed reactor. The lower mass transportability of the large PAHs might induce an increase in the effective residence time in the reactor, yielding more PAHs than were observed experimentally.

The kinetic parameters of the reactions involved in the chemistry of the PAHs were not obtained experimentally and theoretically but rather estimated, based on their prototype reactions of small molecules.[43] Accurate evaluation of the rate of these reactions, as well as further exploration of new routes to PAHs, will be helpful to improve the model predictions of the PAH profiles. Nevertheless, the increasing gap between experimental and computational results with increasing size of the PAH strongly suggests the need for a transport model that describes the flow characteristics in the reactor. Numerical

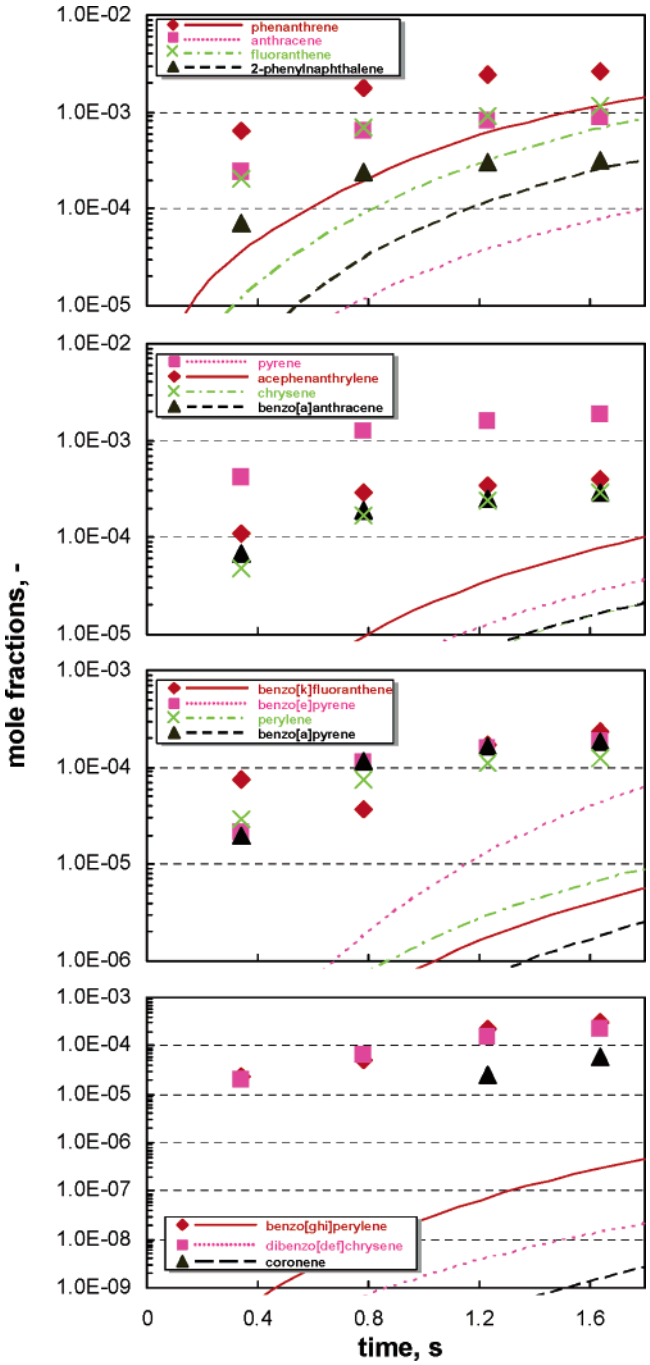

Figure 10. Comparison of model predictions (lines) with experimental mole fraction profiles (symbols) of polycyclic aromatic hydrocarbons (PAHs) during acetylene pyrolysis in a flow reactor at 900 °C and 15 kPa.

simulations with a transport model will identify the reason for the disagreements found in the PAH profiles.

7. Summary

The kinetics of gas-phase reactions during the chemical vapor deposition (CVD) of carbon from ethylene, acetylene, and propylene were modeled using elementary reactions consisting of 227 species and 827 reactions and computed using a time-dependent homogeneous reaction system. Experimental data obtained using a conventional flow reactor were used to validate the model. For the pyrolysis of all three hydrocarbons, satisfactory agreement between the computations and experiments was observed for the major species with mole fractions of $>10^{-2}$. Information about the crucial reaction steps in the formation

and consumption of the major species was obtained by sensitivity and reaction-rate analyses. The influences of pressure and concentration also were predicted well.

Our work describes a single mechanism that has a comprehensive capability to predict the major components found in the pyrolysis of three different hydrocarbons with an acceptable level of accuracy. However, disagreements between the computations and experiments are observed for minor species; in particular, the formation of polycyclic aromatic hydrocarbons (PAHs) is significantly underpredicted. Our lack of understanding of the formation chemistry of PAHs and the lack of flow simulation in our model are likely the major sources of the disagreements. Future work will include studies at different temperatures and surface (deposition) chemistry and with different transport models.

Acknowledgment

This research was performed in the Sonderforschungsbereich (SFB) 551, "Carbon from Gas-Phase: Elementary Reactions, Structures, Materials", which is funded by the Deutsche Forschungsgemeinschaft (DFG). The Alexander von Humboldt Foundation is acknowledged for providing a research fellowship to K.N. The authors thankfully acknowledge the use of the computer program HOMREA by Prof. J. Warnatz (University of Heidelberg). The authors also thank Prof. K. J. Hüttinger (University of Karslruhe) for many fruitful discussions and Dr. H. H. Carstensen (Colorado School of Mines) for his useful comments on the reaction mechanism.

Supporting Information Available: The reaction mechanism and references for each of the elementary reactions (Table S1), species abbreviations and corresponding chemical formulas (Table S2), and thermodynamic data for all species (Table S3). Results of sensitivity analysis (Figures S1−S3) and comparison of model predictions with experimental mole fractions (Figures S4−S9). This material is available free of charge via the Internet at http://pubs.acs.org.

Literature Cited

(1) Savage, G. *Carbon−Carbon Composite*; Chapmann and Hall: London, 1993.

(2) Golecki, I. In *World of Carbon Fibers and Composites*; Delhaes, P., Ed.; Taylor and Francis: London and New York, 2003; Vol. 2, p 112.

(3) Zhang, W. G.; Hüttinger, K. J. Densification of a 2D Carbon Fiber Preform by Isothermal, Isobaric CVI: Kinetics and Carbon Microstructure. *Carbon* **2003**, *41*, 2325.

(4) Jeong, H. J.; Park, H. D.; Lee, J. D.; Park, J. O. Densification of Carbon/Carbon Composites by Pulse Chemical Vapor Infiltration. *Carbon* **1996**, *34*, 417.

(5) Lavenac, J.; Langlais, F.; Feron, O.; Naslain, R. Microstructure of the Pyrocarbon Matrix in Carbon/Carbon Composites. *Compos. Sci. Technol.* **2001**, *61*, 339.

(6) McAllister, P.; Hendricks, J. F.; Wolf, E. E. The Infiltration of Carbon-Fiber Felts and Composites by Pyrolytic Carbon Deposition from Propylene. *Carbon* **1990**, *28*, 579.

(7) McAllister, P.; Wolf, E. E. Modeling of Chemical Vapor Infiltration of Carbon in Porous Carbon Substrates. *Carbon* **1991**, *29*, 387.

(8) McAllister, P.; Wolf, E. E. Simulation of a Multiple Substrate Reactor for Chemical-Vapor Infiltration of Pyrolytic Carbon within Carbon−Carbon Composites. *AIChE J.* **1993**, *39*, 1196.

(9) Bammidipati, S.; Stewart, G. D.; Elliott, J. R.; Gokoglu, S. A.; Purdy, M. J. Chemical Vapor Deposition of Carbon on Graphite by Methane Pyrolysis. *AIChE J.* **1996**, *42*, 3123.

(10) Becker, A.; Hüttinger, K. J. Chemistry and Kinetics of Chemical Vapor Deposition of Pyrocarbon—II. Pyrocarbon Deposition from Ethylene, Acetylene and 1,3-butadiene in the Low Temperature Regime. *Carbon* **1998**, *36*, 177.

(11) Zhang, W. G.; Hüttinger, K. J. Chemical Vapor Infiltration of Carbon—Revised: Part I: Model Simulations. *Carbon* **2001**, *39*, 1013.

(12) Zhang, W. G.; Hüttinger, K. J. Simulation Studies on Chemical Vapor Infiltration of Carbon. *Compos. Sci. Technol.* **2002**, *62*, 1947.

(13) Dean, A. M. Detailed Kinetic Modeling of Autocatalysis in Methane Pyrolysis. *J. Phys. Chem.* **1990**, *94*, 1432.

(14) Dagaut, P.; Cathonnet, M.; Boettner, J. C. Kinetic Modeling of Propane Oxidation and Pyrolysis. *Int. J. Chem. Kinet.* **1992**, *24*, 813.

(15) Dente, M.; Pierucci, S.; Ranzi, E.; Bussani, G. New Improvements in Modeling Kinetic Schemes for Hydrocarbons Pyrolysis Reactors. *Chem. Eng. Sci.* **1992**, *47*, 2629.

(16) Hidaka, Y.; Nakamura, T.; Tanaka, H.; Jinno, A.; Kawano, H.; Higashihara, T. Shock-Tube and Modeling Study of Propene Pyrolysis. *Int. J. Chem. Kinet.* **1992**, *24*, 761.

(17) Broadbelt, L. J.; Stark, S. M.; Klein, M. T. Computer-Generated Pyrolysis Modeling: On-the-Fly Generation of Species, Reactions, and Rates. *Ind. Eng. Chem. Res.* **1994**, *33*, 790.

(18) Tan, Y.; Dagaut, P.; Cathonnet, M.; Boettner, J. C. Pyrolysis, Oxidation and Ignition of C_1 and C_2 Hydrocarbons: Experiments and Modeling. *J. Chim. Phys.* **1995**, *92*, 726.

(19) Hidaka, Y.; Sato, K.; Henmi, Y.; Tanaka, H.; Inami, K. Shock-tube and Modeling Study of Methane Pyrolysis and Oxidation. *Combust. Flame* **1999**, *118*, 340.

(20) Grenda, J. M.; Androulakis, I. P.; Dean, A. M.; Green, W. H. Application of Computational Kinetic Mechanism Generation to Model the Autocatalytic Pyrolysis of Methane. *Ind. Eng. Chem. Res.* **2003**, *42*, 1000.

(21) Matheu, D. M.; Dean, A. M.; Grenda, J. M.; Green, W. H. Mechanism Generation with Integrated Pressure Dependence: A New Model for Methane Pyrolysis. *J. Phys. Chem. A* **2003**, *107*, 8552.

(22) Sheng, C. Y.; Dean, A. M. Importance of Gas-Phase Kinetics within the Anode Channel of a Solid-Oxide Fuel Cell. *J. Phys. Chem. A* **2004**, *108*, 3772.

(23) Matheu, D. M.; Grenda, J. M. A Systematically Generated, Pressure-Dependent Mechanism for High-Conversion Ethane Pyrolysis. 1. Pathways to the Minor Products. *J. Phys. Chem. A* **2005**, *109*, 5332.

(24) Matheu, D. M.; Grenda, J. M. A Systematically Generated, Pressure-Dependent Mechanism for High-Conversion Ethane Pyrolysis. 2. Radical Disproportionations, Missing Reaction Families, and the Consequences of Pressure Dependence. *J. Phys. Chem. A* **2005**, *109*, 5343.

(25) Descamps, C.; Vignoles, G. L.; Feron, O.; Langlais, F.; Lavenac, J. Correlation between Homogeneous Propane Pyrolysis and Pyrocarbon Deposition. *J. Electrochem. Soc.* **2001**, *148*, C695.

(26) Ziegler, I.; Fournet, R.; Marquaire, P. M. Pyrolysis of Propane for CVI of Pyrocarbon: Part I. Experimental and Modeling Study of the Formation of Toluene and Aliphatic Species. *J. Anal. Appl. Pyrolysis* **2005**, *73*, 212.

(27) Ziegler, I.; Fournet, R.; Marquaire, P.-M. Pyrolysis of Propane for CVI of Pyrocarbon: Part II. Experimental and Modeling Study of Polyaromatic Species. *J. Anal. Appl. Pyrolysis* **2005**, *73*, 231.

(28) Norinaga, K.; Hüttinger, K. J. Kinetics of Surface Reactions in Carbon Deposition from Light Hydrocarbons. *Carbon* **2003**, *41*, 1509.

(29) Zhang, W. G.; Hu, Z. J.; Hüttinger, K. J. Chemical Vapor Infiltration of Carbon Fiber Felt: Optimization of Densification and Carbon Microstructure. *Carbon* **2002**, *40*, 2529.

(30) Chevalier, C.; Warnatz, J.; Melenk, H. Automatic-Generation of Reaction-Mechanisms for the Description of the Oxidation of Higher Hydrocarbons. *Ber. Bunsen−Ges.* **1990**, *94*, 1362.

(31) Dimaio, F. P.; Lignola, P. G.; King, A. Kinetic Network Generator. *Chem. Eng. Sci.* **1992**, *47*, 2713.

(32) Broadbelt, L. J.; Stark, S. M.; Klein, M. T. Termination of Computer-Generated Reaction-Mechanisms: Species Rank-Based Convergence Criterion. *Ind. Eng. Chem. Res.* **1995**, *34*, 2566.

(33) Blurock, E. S. Reaction-System for Modeling Chemical Reactions. *J. Chem. Inf. Comput. Sci.* **1995**, *35*, 607.

(34) Prickett, S. E.; Mavrovouniotis, M. L. Construction of Complex Reaction Systems—III. An Example: Alkylation of Olefins. *Comput. Chem. Eng.* **1997**, *21*, 1325.

(35) Glaude, P. A.; Warth, V.; Fournet, R.; Battin-Leclerc, F.; Scacchi, G.; Come, G. M. Modeling of the Oxidation of *n*-Octane and *n*-Decane Using an Automatic Generation of Mechanisms. *Int. J. Chem. Kinet.* **1998**, *30*, 949.

(36) Dong, G. L.; Hüttinger, K. J. Consideration of Reaction Mechanisms Leading to Pyrolytic Carbon of Different Textures. *Carbon* **2002**, *40*, 2515.

(37) Norinaga, K.; Deutschmann, O.; Hüttinger, K. J. Analysis of Gas Phase Compounds in Chemical Vapor Deposition of Carbon from Light Hydrocarbons. *Carbon* **2006**, *44*, 1790.

(38) Wang, H.; Frenklach, M. A Detailed Kinetic Modeling Study of Aromatics Formation in Laminar Premixed Acetylene and Ethylene Flames. *Combust. Flame* **1997**, *110*, 173.

(39) Appel, J.; Bockhorn, H.; Frenklach, M. Kinetic Modeling of Soot Formation with Detailed Chemistry and Physics: Laminar Premixed Flames of C_2 Hydrocarbons. *Combust. Flame* **2000**, *121*, 122.

(40) Marinov, N. M.; Pitz, W. J.; Westbrook, C. K.; Castaldi, M. J.; Senkan, S. M. Modeling of Aromatic and Polycyclic Aromatic Hydrocarbon Formation in Premixed Methane and Ethane Flames. *Combust. Sci. Technol.* **1996**, *116*, 211.

(41) Hidaka, Y.; Higashihara, T.; Ninomiya, N.; Masaoka, H.; Nakamura, T.; Kawano, H. Shock Tube and Modeling Study of 1,3-Butadiene Pyrolysis. *Int. J. Chem. Kinet.* **1996**, *28*, 137.

(42) Tsang, W. Chemical Kinetic Data-Base for Combustion Chemistry. 5. Propene. *J. Phys. Chem. Ref. Data* **1991**, *20*, 221.

(43) Richter, H.; Howard, J. B. Formation and Consumption of Single-Ring Aromatic Hydrocarbons and Their Precursors in Premixed Acetylene, Ethylene and Benzene Flames. *Phys. Chem. Chem. Phys.* **2002**, *4*, 2038.

(44) Tsang, W.; Hampson, R. F. Chemical Kinetic Database for Combustion Chemistry. 1. Methane and Related-Compounds. *J. Phys. Chem. Ref. Data* **1986**, *15*, 1087.

(45) Sato, K.; Hidaka, Y. Shock-Tube and Modeling Study of Acetone Pyrolysis and Oxidation. *Combust. Flame* **2000**, *122*, 291.

(46) Burcat, A.; Ruscic, B. Third Millennium Ideal Gas and Condensed Phase ThermoChemical Database for Combustion with updates from Active ThermoChemical Tables. ANL-05/20 and TAE 960 Technion-IIT, Aerospace Engineering, and Argonne National Laboratory, Chemistry Division, September 2005.

(47) Warnatz, J.; Maas, U.; Dibble, R. W. *Combustion*; 3rd Edition; Springer−Verlag: Heidelberg, New York, 2000.

(48) Deutschmann, O.; Tischer, S.; Correa, C.; Chatterjee, D.; Kleditzsch, S.; Janardhanan, V.; DETCHEM 2.0, Karlsruhe 2004 (Available via the Internet at http://www.detchem.com).

(49) Bergmann, U.; Lummer, K.; Atakan, B.; Kohse-Hoinghaus, K. Flame Deposition of Diamond Films: An Experimental Study of the Effects of Stoichiometry, Temperature, Time and the Influence of Acetone. *Ber. Bunsen−Ges.* **1998**, *102*, 906.

(50) Duran, R. P.; Amorebieta, V. T.; Colussi, A. J. Lack of Kinetic Hydrogen Isotope Effect in Acetylene Pyrolysis. *Int. J. Chem. Kinet.* **1989**, *21*, 847.

(51) Wang, H.; Frenklach, M. Calculations of Rate Coefficients for the Chemicaly Activated Reactions of Acetylene with Vinylic and Aromatic Radicals. *J. Phys. Chem.* **1994**, *98*, 11465.

(52) Hidaka, Y.; Higashihara, T.; Ninomiya, N.; Oshita, H.; Kawano, H. Thermal-Isomerization and Decomposition of 2-Butyne in Shock-Waves. *J. Phys. Chem.* **1993**, *97*, 10977.

(53) Tabayashi, K.; Bauer, S. H. Early Stages of Pyrolysis and Oxidation of Methane. *Combust. Flame* **1979**, *34*, 63.

(54) Hidaka, Y.; Higashihara, T.; Ninomiya, N.; Oki, T.; Kawano, H. Thermal-Isomerization and Decomposition of 1,2-Butadiene in Shock-Waves. *Int. J. Chem. Kinet.* **1995**, *27*, 331.

(55) Westmoreland, P. R.; Dean, A. M.; Howard, J. B.; Longwell, J. P. Forming Benzene in Flames by Chemically Activated Isomerization. *J. Phys. Chem.* **1989**, *93*, 8171.

(56) Orchard, S. W.; Thrush, B. A. Photochemical Studies of Unimolecular Processes. 6. Unimolecular Reactions of C_6H_8 Isomers and Interpretation of Their Photolyses. *Proc. R. Soc. London Ser. A−Math. Phys. Eng. Sci.* **1974**, *337*, 257.

(57) Emdee, J. L.; Brezinsky, K.; Glassman, I. A Kinetic-Model for the Oxidation of Toluene near 1200-K. *J. Phys. Chem.* **1992**, *96*, 2151.

(58) Mebel, A. M.; Lin, M. C.; Yu, T.; Morokuma, K. Theoretical Study of Potential Energy Surface and Thermal Rate COnstants for the $C_6H_5 + H_2$ and $C_6H_6 + H$ Reactions. *J. Phys. Chem. A* **1997**, *101*, 3189.

(59) Hidaka, Y.; Nakamura, T.; Miyauchi, A.; Shiraishi, T.; Kawano, H. Thermal-Decomposition of Propyne and Allene in Shock-Waves. *Int. J. Chem. Kinet.* **1989**, *21*, 643.

(60) Fournet, R.; Bauge, J. C.; Battin-Leclerc, F. Experimental and Modeling of Oxidation of Acetylene, Propyne, Allene and 1,3-butadiene. *Int. J. Chem. Kinet.* **1999**, *31*, 361.

(61) Chanmugathas, C.; Heicklen, J. Pyrolysis of Acetylene−Vinylacetylene Mixtures between 400 °C and 500 °C. *Int. J. Chem. Kinet.* **1986**, *18*, 701.

(62) Fahr, A.; Stein, S. E. Reactions of Vinyl and Phenyl Radicals with Ethyne, Ethene and Benzene. *Proc. Combust. Inst.* **1988**, *22*, 1023.

(63) Zhong, X.; Bozzelli, J. W. Thermochemical and Kinetic Analysis of the H, OH, HO_2, O, and O_2 Association Reactions with Cyclopentadienyl Radical. *J. Phys. Chem. A* **1998**, *102*, 3537.

(64) Rao, V. S.; Skinner, G. B. Study of the High-Temperature Pyrolysis of Propene by Determination of H Atoms and D Atoms Formed from Partially Deuterated Propenes Heated Behind Shock-Waves. *J. Phys. Chem.* **1989**, *93*, 1869.

(65) Dean, A. M. Predictions of Pressure and Temperature Effects Upon Radical-Addition and Recombination Reactions. *J. Phys. Chem.* **1985**, *89*, 4600.

(66) Tsang, W. Chemical Kinetic Data-Base for Combusttion Chemistry. 3. Propane. *J. Phys. Chem. Ref. Data* **1988**, *17*, 887.

(67) Weissman, M.; Benson, S. W. Mechanism of Soot Initiation in Methane Systems. *Progress Energy Combust. Sci.* **1989**, *15*, 273.

(68) Heyberger, B.; Belmekki, N.; Conraud, V.; Glaude, P. A.; Fournet, R.; Battin-Leclerc, F. Oxidation of Small Alkenes at High Temperature. *Int. J. Chem. Kinet.* **2002**, *34*, 666.

Received for review September 15, 2006
Revised manuscript received February 16, 2007
Accepted March 7, 2007

IE061207P